

Influence of silica content in sulfonated poly(arylene ether ether ketone ketone) (SPAEKK) hybrid membranes on properties for fuel cell application[☆]

Dae Sik Kim, Baijun Liu, Michael D. Guiver^{*}

Institute for Chemical Process and Environmental Technology, National Research Council of Canada, Ottawa, Ontario K1A 0R6, Canada

Received 31 May 2006; received in revised form 22 August 2006; accepted 1 September 2006

Available online 29 September 2006

Abstract

Sulfonated poly(arylene ether ether ketone ketone) (SPAEKK) copolymer containing pendant sulfonic acid group (sulfonic acid content (SC) = 0.67) was synthesized from commercially available monomers such as sodium 6,7-dihydroxy-2-naphthalenesulfonate (DHNS), 1,3-bis(4-fluorobenzoyl)-benzene (BFBB), and hexafluorobisphenol A (6F-BPA). SPAEKK/silica hybrid membranes were prepared using the sol–gel process under acidic conditions. The SPAEKK/silica hybrid membranes were fabricated with different silica contents and the membranes were modified to achieve improved proton conductivity incorporating P–OH groups (H_3PO_4 treatment).

The silica particles within the membranes were used for the purpose of blocking excessive methanol cross-over and for forming a pathway for proton transport due to water absorption onto the hydrophilic $\equiv\text{SiOH}$ surface. The proton conductivities of H_3PO_4 -doped membranes were somewhat higher than the un-doped (H_3PO_4 -free) membranes due to increasing hydrophilicity of the membranes. The presence of silica particles within the organic polymer matrix, which decreases the ratio of free water to bound water due to the $\equiv\text{SiOH}$ on the surface of silica derived from sol–gel reaction, results in hybrid membranes with reduced methanol permeability and improved proton conductivity.

Crown Copyright © 2006 Published by Elsevier Ltd. All rights reserved.

Keywords: Sulfonated poly(arylene ether ether ketone ketone); Sol–gel process; Proton conductivity

1. Introduction

Direct methanol fuel cells (DMFCs) are being developed as a portable power source for various kinds of mobile electronics because they can utilize methanol without reforming equipment of methanol to hydrogen gas [1]. The heart of the fuel cell is the polymer electrolyte membrane (PEM) whose essential function is as a proton conductive medium as well as a barrier to avoid the direct contact between fuel and oxidant [2]. The commercial Nafion membranes such as the fluorinated membrane from DuPont, Flemion from Asahi Glass and

Neosepta from Tokuyama Soda have been intensively used as proton-conducting electrolyte membranes due to their chemical stability and high proton conductivity (~ 0.1 S/cm) in the fully hydrated state [3,4]. However, the operational limit of these polymers is usually considered to be about 100 °C or lower because of the deterioration of proton transport and mechanical and electrochemical properties [5]. Additionally Nafion easily expands or shrinks depending on the humidity of the environment [6]. Methanol permeation is usually greatly increased by expansion of polymer due to absorption of methanol by the polymer itself [7]. Nafion membrane has high methanol permeability ($\sim 10^{-6}$ cm²/s) which drastically reduced the DMFC's performance [8]. One of the challenges in current DMFC research is the development of novel proton conductive membranes for improving the performance of DMFC by improving the proton conductivity and reducing the methanol permeability.

[☆] NRCC Publication 49104.

^{*} Corresponding author. Institute for Chemical Process and Environmental Technology, National Research Council of Canada, Building M-12, Room 245, 1200 Montreal Road, Ottawa, Ontario K1A 0R6, Canada. Tel.: +1 613 993 9753; fax: +1 613 991 2384.

E-mail address: michael.guiver@nrc-cnrc.gc.ca (M.D. Guiver).

The electrochemical properties of the materials are strongly dependent on the chemical structure of the polymer. In particular, the hydrophilic domain structures of the membranes under hydrated conditions play an important role in proton and methanol transport [9]. These domains form ionic channels, the size of which needs to be reduced while maintaining proton conductivity to obtain low methanol permeability; this can be achieved by controlling the structure of the ionic channels and the state of water in the membrane.

One of the several approaches is the incorporation of inorganic components into membranes. Mauritz et al. have reported on a novel Nafion/silica hybrid membrane, which is made by a sol–gel reaction of tetraethoxysilane (TEOS) to form silica inside a Nafion membrane [10]. Deng et al. reported that the incorporation of silica enhanced the hydrophilicity of clusters in Nafion, and this effect was attributed to the presence of numerous $\equiv\text{SiOH}$ groups to which H_2O molecules can hydrogen bond [11]. It is reported that the presence of silica particles in the organic polymer matrix results in hybrid membranes with markedly reduced methanol permeabilities [12]. Kuo et al. reported a new type of organic–inorganic hybrid polymer electrolyte comprising *ortho*-phosphoric acid (H_3PO_4) as a proton donor for medium-temperature applications through the sol–gel method [13].

Inexpensive engineering thermoplastics, such as poly(ether ether ketone) (PEEK) [14], polysulfone (PSf) [15] and polybenzimidazole (PBI) [16], are being evaluated as alternatives to Nafion membranes for PEM fuel cell application. PEEK is very promising since it possesses good mechanical properties and high thermal stability. PEEK can be converted to sulfonated PEEK by electrophilic substitution of the sulfonic acid groups in the polymer backbone. Meng et al. synthesized aromatic poly(arylene ether)s containing pendant sulfonic acid groups. The rationale for this is to reduce hydrolytic and oxidative degradation [17–20].

Compared to perfluorinated sulfonic acid membranes, sulfonated poly(aryl ether ketone) is reported to have a smaller characteristic separation length and wider distribution of the proton-conducting channels with more dead-end channels and a larger internal interface between the hydrophobic and hydrophilic domains [21]. If short pendant side chains exist in the polymer structure, the nanophase separation of hydrophilic and hydrophobic domains may be improved [22]. Recently, we reported the syntheses of series of poly(arylene ether ether ketone ketone) copolymers containing pendant sulfonic acid groups bonded to naphthalene from commercially available sodium 6,7-dihydroxy-2-naphthalenesulfonate (DHNS), 1,3-bis(4-fluorobenzoyl)-benzene (BFBB) and 4,4'-biphenol or hydroquinone [23].

The objective of this study is the evaluation of proton conductivity and methanol permeability of the SPAEEKK/silica hybrid membrane. To do this, DHNS was used to prepare the poly(arylene ether ether ketone ketone) copolymer containing sulfonic acid groups (SPAEEKK) via nucleophilic polycondensation with commercially available monomers BFBB and 6F-BPA, following a procedure we used to prepare a similar

polymer previously [23]. 6F-BPA was incorporated in place of previously used 4,4'-biphenol or hydroquinone to impart more flexibility into the polymer. Silica content from 5 to 15 wt% was introduced into the polymer matrix using the sol–gel process under acidic conditions. We also report the preparation of hybrid membranes, in which only surfaces of SPAEEKK/silica membranes were modified to achieve improved proton conductivity by incorporating P–OH groups (H_3PO_4 treatment). The transport properties, such as proton conductivity and methanol permeability, in relation to the state of water in the membrane were measured to evaluate their potential as feasible PEM for fuel cell applications.

2. Experimental

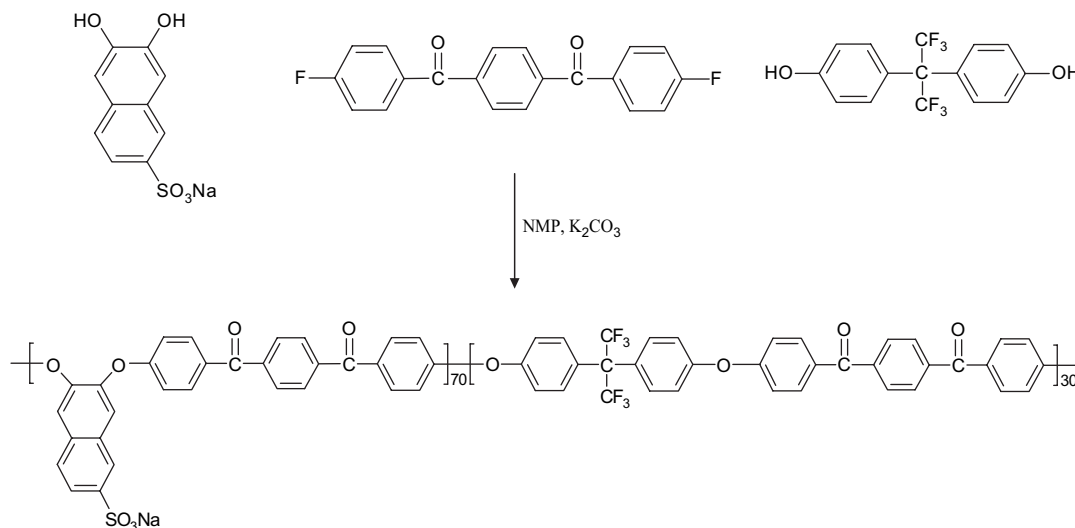
2.1. Chemicals and materials

Sodium 6,7-dihydroxy-2-naphthalenesulfonate (DHNS) was purchased from Rintech, Inc. and recrystallized from a mixture of ethanol/water (50/50 v/v) before use. 1,4-Bis(4-fluorobenzoyl)benzene (1,4-BFBB, Jilin University, China) and hexafluorobisphenol A (6F-BPA, Sigma–Aldrich, Co.) were recrystallized from 1,2-dichlorobenzene and toluene, respectively. Tetraethyl orthosilicate (TEOS), methanol (MeOH) and H_3PO_4 were of analytical grade from Sigma–Aldrich Co. All other chemicals (obtained from Sigma–Aldrich) were of reagent grade and used as received.

2.2. Synthesis of poly(arylene ether ether ketone ketone)s and hybrid membranes

Following a procedure for preparing a similar polymer reported previously [23], DHNS was polymerized with 6F-BPA and BFBB as shown in Scheme 1. A typical synthetic procedure to prepare sulfonated copolymers (DHNS/6F-BPA = 70/30) is described as follows. Compounds 10 mmol 1,4-BFBB, 7 mmol DHNS, 3 mmol 6F-BPA, and 15 mmol K_2CO_3 were added into a three-necked flask equipped with a magnetic stirrer, a Dean–Stark trap, and an argon gas inlet. Then, 15 ml NMP and 15 ml toluene were charged into the reaction flask under argon atmosphere. The reaction mixture was heated to 140–150 °C. After dehydration and removal of toluene, the reaction temperature was gradually increased to 180 °C. When the solution viscosity increased significantly, the mixture was cooled to 100 °C and coagulated into a large excess of ethanol or water with vigorous stirring. The precipitated copolymer (SPAEEKK-70) was washed several times with water and dried in a vacuum oven at 90 °C for 24 h. The yield of polymer was >90%.

Inorganic–organic hybrids were prepared by the addition of TEOS solution to a filtered solution of SPAEEKK-70 in DMAc. The TEOS solution was prepared by mixing H_2O /TEOS/HCl in a mole ratio of 4/1/0.1. The solution was stirred at room temperature for 2 h. The amount of TEOS was 5%, 10% and 15% by weight to SPAEEKK weight. After hydrolysis, the mixture became a clear silica sol. The solution containing silica sols was mixed together with SPAEEKK solution



Scheme 1. Synthesis of SPAEEKK copolymers.

and stirred for 12 h at room temperature under N_2 gas. This solution was poured onto a glass plate and dried at $60^\circ C$ under a constant purge of N_2 over 3 days.

The hybrid membranes were dried at $80^\circ C$, followed by immersion in 5% H_3PO_4 solutions for 10 h at $70^\circ C$ to incorporate P–OH group. The membrane was washed and immersed in deionized water for more than 12 h at room temperature to remove excess acid.

The nomenclature used for membranes described in this article is as follows. SP/Si *xx* and SP/Si/POH *xx* relate to SPAEEKK/silica hybrid membranes and post-treated ones, respectively, where *xx* refers to weight percentage of TEOS relative to SPAEEKK copolymer.

2.3. Characterization of SPAEEKK membrane and hybrid membranes

The SPAEEKK membranes were analyzed by Fourier transform infrared (FT-IR, Nicolet Model Magna IR 550, Madison, WI, USA) spectroscopy. 1H NMR spectra were obtained on a Varian Unity Inova NMR spectrometer operating at a proton frequency of 399.95 MHz. Deuterated dimethyl sulfoxide ($DMSO-d_6$) was the NMR solvent, and the DMSO signal at 2.50 ppm was used as the chemical shift reference.

To investigate the morphology of the membranes, fracture surfaces were investigated with a field emission scanning electron microscope (FE-SEM, Jeol Model JSF 6340F, Tokyo, Japan).

The degradation process and the thermal stability of the samples were investigated using thermogravimetry analysis (TGA) (TA Instruments, TGA 2950). The TGA measurements were then carried out under a nitrogen atmosphere using a heating rate of $10^\circ C/min$ from 50 to $700^\circ C$.

2.4. Water state, IEC value

The total water content (%) was measured as follows. After soaking the membranes in distilled water for more than 24 h,

they were wiped with filter paper and weighed immediately. The membranes were then dried at $100^\circ C$ under a vacuum condition until a constant weight was obtained. The water content (%) by weight is the ratio of the hydrated membrane to the dried membrane.

The non-freezing water content of the membranes in the fully hydrated state was determined by DSC measurement. A hydrated hybrid membrane was hermetically sealed in a sample pan. The DSC module was purged with nitrogen gas and quenched down to $-30^\circ C$ with liquid nitrogen, then heated to $+120^\circ C$ and the transitions were observed.

The ion-exchange capacity (IEC, in mmol/g) values were measured using a classical titration method (ASTM D2187) with 0.01 M NaOH and phenolphthalein (titration indicator).

2.5. Proton conductivity and methanol permeability

Proton conductivity measurements were performed on the SPAEEKK membrane by an ac impedance spectroscopy over a frequency range of $10-10^7$ Hz with an oscillating voltage of 50–500 mV, using a system based on a Solatron 1260 gain phase analyzer. A 20×10 mm membrane sample was placed in a temperature controlled cell open to air by a pinhole where the sample was equilibrated at 100% RH at ambient atmospheric pressure and clamped between two stainless steel electrodes. The conductivities (σ) of the samples were measured in the longitudinal direction and were calculated from the impedance data, using the following relationship

$$\sigma = l/RS \quad (1)$$

where σ is the proton conductivity (in S/cm), l is the distance between the electrodes used to measure the potential ($l = 1$ cm), $S (= W \times d, W = \text{width}, d = \text{thickness})$ is the surface area required for a proton to penetrate the membrane (in cm^2) and R is derived from the low intersection of the high frequency semicircle on a complex impedance plane with the $Re(Z)$ axis.

2.6. Methanol permeability

The permeability experiments were carried out utilizing a glass diffusion cell. One compartment of the cell ($V_A = 100$ ml) was filled with a solution of methanol (10 vol.%) and 1-butanol (0.2 vol.%) in deionized water. The other ($V_B = 100$ ml) was filled with 1-butanol (0.2 vol.%) solution in deionized water. The membrane was clamped between the two compartments and both of these were kept under stirring during the experiment. A flux of methanol sets up across the membrane as a result of the concentration difference between the two compartments. A detailed description of the experimental set-up and procedure can be found elsewhere [24]. The methanol concentration in the receiving compartment as a function of time is given by

$$C_B(t) = \frac{A}{V_B} \frac{DK}{L} C_A(t - t_0) \quad (2)$$

where C_B and C_A are the two methanol concentrations; A and L are the membrane area and thickness; D and K are the methanol diffusivity and partition coefficient between the membrane and the adjacent solution. Assumptions are made here that D inside the membrane is constant and K does not depend on concentration. The product DK is the membrane permeability. t_0 , also termed as time lag, is explicitly related to the diffusivity: $t_0 = L^2/6D$ [25]. C_B is measured several times during an experiment and the permeability is calculated from the slope of the straight line. Methanol concentrations were determined by ^1H NMR spectroscopy using solutions taken directly from the diffusion cell without the use of deuterated solvents. Shimming was done using the ^1H resonance of H_2O . 1-Butanol in D_2O was used as the internal reference standard.

During permeability tests the temperature was controlled at 30 and 80 °C by means of a thermostatic water bath.

3. Results and discussion

3.1. Synthesis and characterization of SPAEEKK and hybrid membranes

All monomers used in this study for the preparation of SPAEEKK/silica hybrid membranes are commercially available and are inexpensive. The functional monomer DHNS is a naphthalene diol with a pendant sodium sulfonate group. Since DHNS has a tendency for oligomer formation by cyclization, it is necessary to use the longer difluorodiketone monomer 1,3-BFBB in place of the often used 4,4'-difluorodiphenyl ketone monomer. The comonomers 4,4'-biphenol and hydroquinone were selected for copolymerization with 1,3-BFBB in our previous study [23]. In this study, DHNS, 1,4-BFBB, and 6F-BPA were polymerized in NMP and toluene was used to remove the water from starting materials and that formed during the reactions as shown in Scheme 1. The 6F-BPA monomer was utilized to impart more flexibility into the polymer chain. The sulfonic acid groups are attached on DHNS away from the ether linkage, which is expected to decrease the effect on the hydrolysis of ether linkages [23].

Aromatic protons located at the electron-rich *ortho*-ether position of 6F-BPA and 1,3-BFBB are shielded and appear at low frequency (7.0–7.3 ppm) while the H_4 proton *ortho* to sulfonate group on the pendant naphthalene is the most deshielded and appears at high frequency as shown in Fig. 1. The sulfonation content (SC) is expressed as the ratio of DHNS units (bearing the $-\text{SO}_3\text{Na}$ group) to 1.0 BFBB unit.

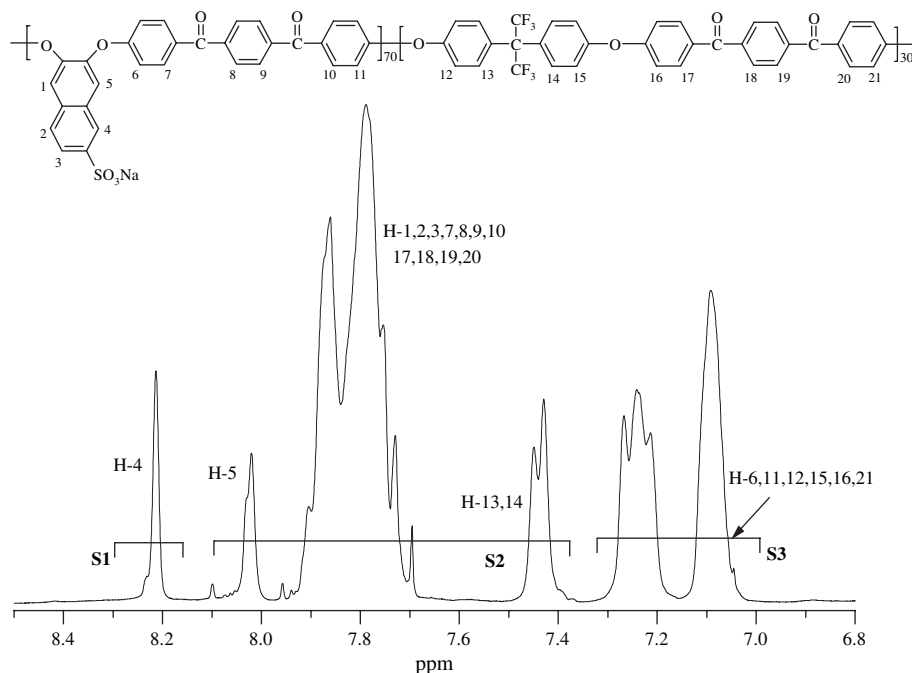


Fig. 1. ^1H NMR spectra of SPAEEKK copolymers.

^1H NMR spectroscopy was the most convenient method to determine the experimentally obtained SC from the copolymerization reactions [23]. The aromatic region of the polymer was split into three sections (S1, S2, and S3) and their integral values were used in the calculation of the SC using the following equation:

$$\frac{S1}{S3} = \frac{(n)}{(8-4n)} \text{ or } \frac{S2}{S3} = \frac{(12)}{(8-4n)}$$

where

$$\begin{aligned} S1 & (8.14\text{--}8.3 \text{ ppm, integral values} = 0.66) = H_4 \times n = n \\ S2 & (7.34\text{--}8.06 \text{ ppm, integral values} = 12.11) = H_{1,2,3,5} \times n + H_{7,8,9,10} + H_{13,14}(1-n) = 12 \\ S3 & (6.92\text{--}7.34 \text{ ppm, integral values} = 5.24) = H_{6,11} + H_{12,15}(1-n) = 8 - 4n \\ n & = \text{SC, where } n \text{ refers to the percentage content of aromatic phenol monomers.} \end{aligned}$$

Based on monomer feed ratios, the expected SC of the SPAEEKK used in this study is 0.7. The experimentally determined SC from ^1H NMR data is 0.67. This polymer was used to prepare hybrid membranes.

Fig. 2 shows the FT-IR spectra of the membranes. The membranes show a characteristic band at 1630 cm^{-1} (characteristic of the Ar-C=O stretching), and at 1245 cm^{-1} (characteristic of the C-O-C stretching vibration) [26]. The FT-IR spectra of a series of SPAEEKK membranes had absorption bands at 1048 cm^{-1} (characteristic of the symmetric SO_3H stretching). Therefore, it is clear that the spectral data support the presence of sulfonic acid groups in the copolymers. In addition, new broad bands appear at 1090 cm^{-1} (characteristic of the Si-O-Si asymmetric stretching) in sulfonated hybrid membranes, arising from the products of the sol-gel reaction. The broad absorption peak at around 3400 cm^{-1} in the hybrid membranes indicates that there were a significant number of -OH groups due to non-condensed $\equiv\text{SiOH}$. It is known that the position of the OH absorption bands depends on the

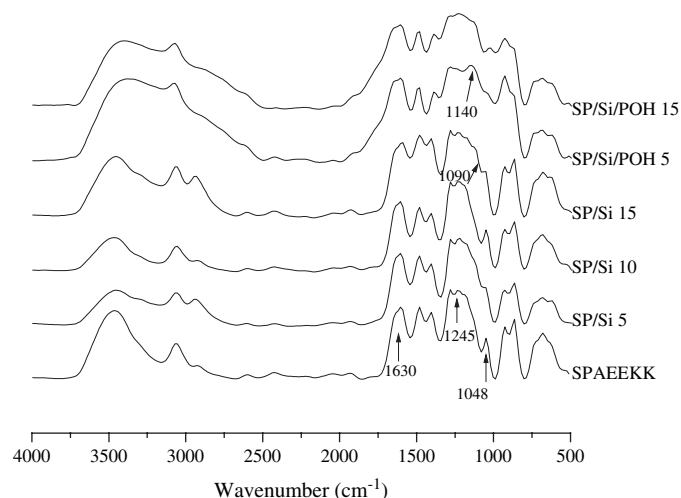


Fig. 2. FT-IR spectra of SPAEEKK/silica hybrid membranes.

degree of strength of hydrogen bonding, and shifts to lower wavenumber with increasing strength of the hydrogen bonding [27]. We suppose that these -OH groups provide the sites for hydrogen bonding with water molecules, because silica nanoparticles have been observed to retain water, even at high temperatures [28]. The broad absorption peak at around $2500\text{--}3500 \text{ cm}^{-1}$ in the hybrid membranes with H_3PO_4 doping indicates that the hydrogen bond interaction occurs among O atoms of C=O in the polymer matrix and $\equiv\text{SiOH}$ and phosphoric acids. In addition, the absorption peak at 2800 cm^{-1} in the hybrid membranes with H_3PO_4 doping indicates OH stretching in O=P-OH group [29]. It is likely that the band at 1140 cm^{-1} arise from P-O-Si stretching [29].

3.2. Thermal properties

The TGA curves measured under flowing nitrogen are shown in Fig. 3. Membrane samples for TGA analysis were preheated to $150 \text{ }^\circ\text{C}$ at $10 \text{ }^\circ\text{C}/\text{min}$ under nitrogen atmosphere and held isothermally for 60 min for moisture removal. The first weight loss region (occurring between temperatures $T=280 \text{ }^\circ\text{C}$ and $T=450 \text{ }^\circ\text{C}$) is assumed to result from the desulfonation. In the second weight loss region, the polymer residues were further degraded at $T=550 \text{ }^\circ\text{C}$, which corresponds to the decomposition of the SPAEEKK main chain. Fig. 3 shows that the thermal stability of the sulfonated groups is enhanced by neutralization (Na form).

In the case of the hybrid composite membranes, the weight remaining after the polymer decomposition depended on the content of the inorganic component. That is, the weight residues of the SP/Si 5, 10, 15 hybrid membranes containing silica at $T=700 \text{ }^\circ\text{C}$ were higher than that of unfilled SPAEEKK membrane. These results suggest that the introduction of silica into the SPAEEKK chains enhances the thermal stability of the given hybrid materials. The increase in the thermal stability may have resulted from the high thermal stability of silica and the crosslink point nature of the silica particles [30].

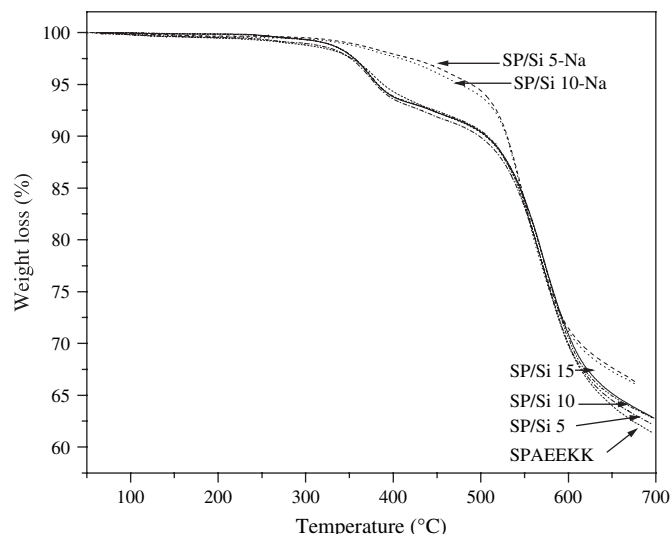


Fig. 3. TGA of SPAEEKK/silica hybrid membranes.

3.3. Morphology

Fig. 4 shows SEM images of the hybrid membranes, showing the silica domains that were observed. The average size of the silica particles was <100 nm. Colloidal silica nanoparticles show great compatibility with organic polymers [31]. The silica added to the polymer solution led to good adhesion between organic and inorganic phases. The silica particles in the hybrid membrane containing the lower silica content (5%) show less uniformity in their distribution. However, the particles in the SP/Si 15 hybrid membrane show uniform distribution. Of further interest in Fig. 4 is that the ratio of P/S decreased from the center to the edge of silica particles. This result is indicative of the phosphoric acid reacting with $\equiv\text{SiOH}$. This interaction of silica and phosphoric acid will affect the surface morphology, the water content, the proton conductivity, and the methanol permeability.

3.4. IEC value and state of water

The IEC value of the sulfonated PAEEKK membrane was 1.30 mmol/g dry membrane, and the hybrid membranes have almost the same IEC values, as shown in Table 1. The total water contents increase with TEOS content and temperature. The introduction of silica enhanced the membrane hydrophilicity due to the presence of numerous $\equiv\text{SiOH}$ groups. These $\equiv\text{SiOH}$ groups, which can hydrogen bond, have strong bonding with H_2O molecules. In addition, the H_3PO_4 -doped membranes (SP/Si/POH xx) show a similar or somewhat higher water content behavior than that of H_3PO_4 -free hybrid

membranes (SP/Si xx). As listed in Table 1, the water content of the SPAEEKK membrane derived from 6F-BPA is lower than that of the previously reported SPAEEKK membranes derived from 4,4'-biphenol or hydroquinone monomer, because of the hydrophobic nature of the 6F-BPA connecting units [23].

It is reported that an important reason for the higher methanol permeability for Nafion is its higher fraction of freezing bound and free water versus non-freezing bound water compared with that of the poly(arylene ether)-based copolymers [32]. It is important to know the state of water in the membrane because the proton conductivity strongly depends on the water content. The water state was measured using a DSC as shown in Fig. 5. A single peak around 0°C is the response for an endothermic peak corresponding to the heat of fusion of free water. The amount of free water was obtained by the integration of the endothermic peak area; then, the amount of bound water was calculated from the difference between the amount of free water and total water. Quantification of each state of water by DSC is obviously of great interest but is difficult because of two overlapping melting peaks. In some cases, bound water can be classified into freezing bound water and non-freezing bound water, which is due to a weak or a strong interaction, respectively, between the water molecules and the polymeric matrix with polar and ionic groups [33]. Table 2 summarizes the amount of free water, bound water, and the ratio of bound and free water per total water. The difference value (Δ) of Nafion 117 is higher than that of SPAEEKK and hybrid membranes. A high Δ means that the water molecules exist in the freezing water state rather than

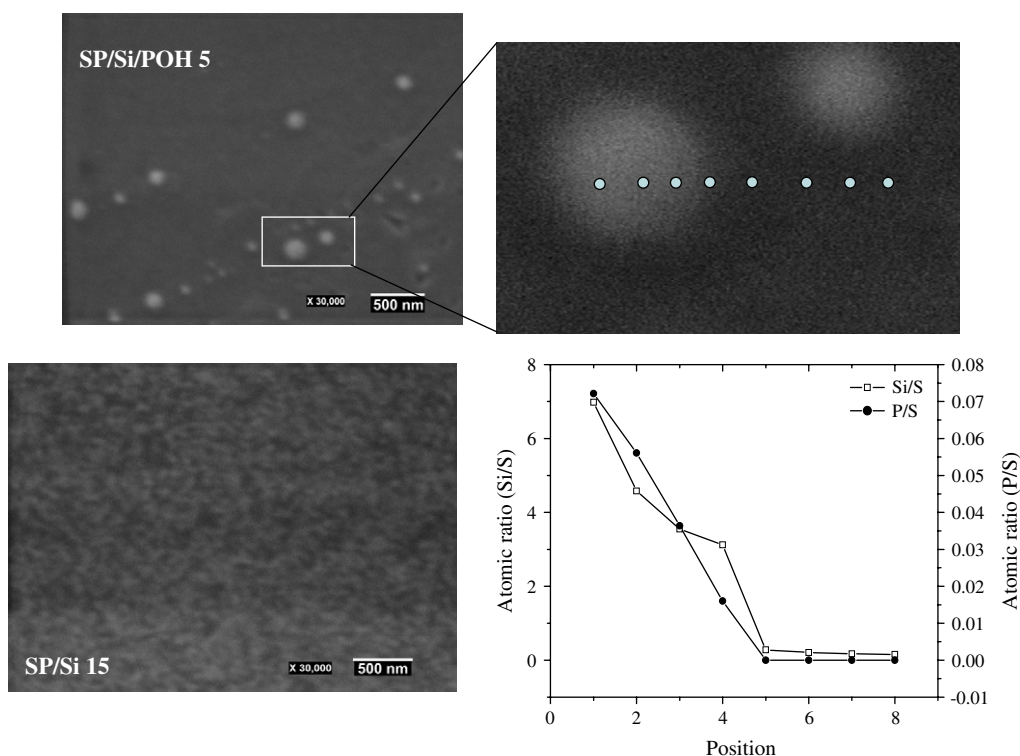


Fig. 4. SEM images of SPAEEKK/silica membranes' surface and elemental concentration ratio of P/Si of the hybrid membrane measured by EDS.

Table 1
Properties of SPAEEKK hybrid membranes

Polymer	Water uptake (%)		λ [H ₂ O]/[SO ₃ H]		Proton conductivity (S/cm)		Meq g/mol SO ₃	IEC
	30 °C	80 °C	30 °C	80 °C	30 °C	80 °C		
SPAEEKK	21.4	26.8	9.1	11.5	0.0186	0.0461	769	1.30
SP/Si 5	23.5	27.9	10.0	11.9	0.0205	0.0485	—	1.30
SP/Si 10	25.3	30.9	11.0	13.4	0.0268	0.0576	—	1.28
SP/Si 15	28.0	33.7	12.4	15.0	0.0297	0.0679	—	1.25
SP/POH	23.5	28.5	10.0	10.9	0.0181	0.0467	—	1.30
SP/Si/POH 5	25.5	30.9	11.0	12.2	0.0246	0.0562	—	1.29
SP/Si/POH 10	27.5	33.5	11.9	13.3	0.0276	0.0657	—	1.28
SP/Si/POH 15	30.2	35.2	13.3	14.5	0.0320	0.0782	—	1.26
SPAEEKK-B70 ^a	24.2	28.3	10.7	15.5	0.0252	0.0392	788	1.26
SPAEEKK-H70 ^a	20.5	33.4	8.6	14.1	0.0275	0.044	756	1.32

^a SPAEEKK copolymer derived from 4,4'-biphenol or hydroquinone monomer (proton conductivity data from Ref. [23] that was originally measured in the transverse mode was re-measured in the longitudinal mode for direct comparison to the present work).

in the bound water state [24]. As listed in Table 2, the bound water increased with increasing silica content. This implies that the bound water can be captured around the silica particles as well as around the sulfonic acid groups. This effect was attributed to the presence of numerous ≡SiOH groups and/or phosphoric acid to which H₂O molecules can hydrogen bond, and this physically absorbed water should be driven off at a higher temperature as compared to H₂O in –SO₃H–H₂O bonds [10]. In addition, another endothermic peak at around 100 °C was observed, indicating the heat of vaporization of the water molecules. The increase of the silica content also caused an increase of the vaporization temperature, which indicated stronger water–polymer interactions due to the existence of more bound water content [33]. Therefore, we expect that the proton conductivity of hybrid membranes is maintained at higher temperature because the hybrid membranes will retain water content by bound water.

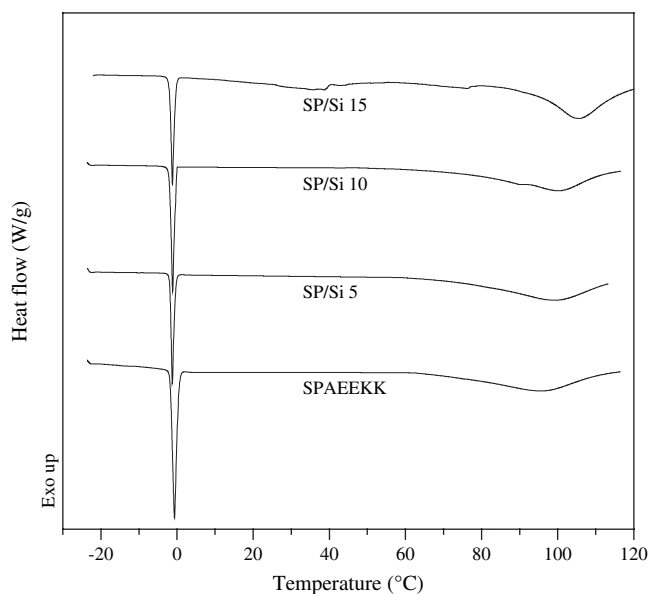


Fig. 5. DSC results indicating the fusion and vaporization temperatures of water in the hydrated membranes.

3.5. Proton conductivity and methanol permeability

Fig. 6 illustrates a schematic representation of a model involved in proton-conduction mechanism and the state of water in the hybrid membrane. Generally, two principal mechanisms describe proton diffusion through the membranes [34]. One is the vehicle mechanism whereby a proton combines with vehicles such as H₃O⁺ or CH₃OH₂⁺ and also with unprotonated vehicles (H₂O), thus allowing the net transport of protons [34]. In this mechanism, the conductivity is directly dependent on the rate of vehicle diffusion. The other is the Grotthuss mechanism (hopping) whereby protons are transferred from one proton acceptor site to another by hydrogen bonds. In this mechanism, additional reorganization of the proton environment, consisting of reorientation of individual species or even more extended ensembles, then it results in the formation of an uninterrupted trajectory for proton migration [34]. Therefore, as shown in Fig. 6, it is probable that the non-freezing and the freezing bound water participate by the Grotthuss mechanism, and the free water takes part by a vehicle mechanism as well as by the Grotthuss mechanism. The free water is evaporated with increasing temperature and consequently the

Table 2
Characterization of water content and fraction of each state of water in the membranes

Polymer	Water content % (at 30 °C)			Ratio (%)		Δ^a
	Total	Free	Bound	[Free]/[Total]	[Bound]/[Total]	
Nafion 117 ^b	23.0	17.1	5.9	74.0	26.0	49.0
SPAEEKK	21.4	9.6	11.8	44.9	55.1	10.3
SP/Si 5	23.5	9.5	14	40.4	59.6	19.1
SP/Si 10	25.3	9.8	15.5	38.7	61.3	22.5
SP/Si 15	28.0	9.2	18.8	32.9	67.1	34.3
SP/POH	23.5	10.9	12.6	46.4	53.6	7.2
SP/Si/POH 5	25.5	11.5	14.0	45.1	54.9	9.8
SP/Si/POH 10	27.5	11.5	16.0	41.8	58.2	16.4
SP/Si/POH 15	30.2	11.8	18.4	39.1	60.9	21.9

^a $\Delta = [\text{Bound}]/[\text{Total}] - [\text{Free}]/[\text{Total}]$.

^b Data from Ref. [24].

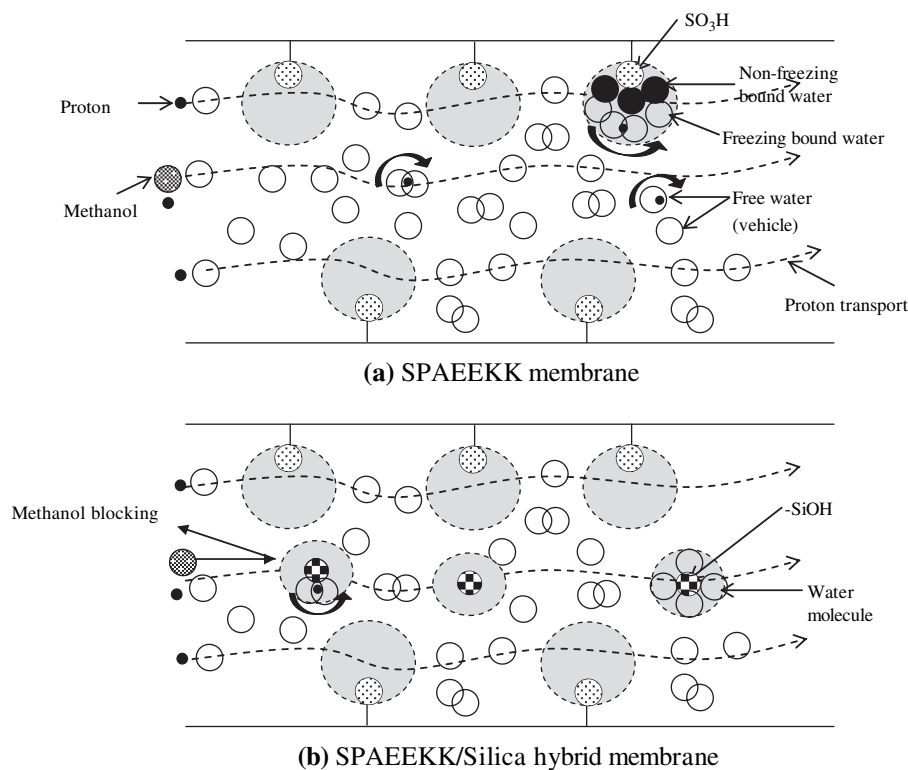


Fig. 6. Schematic representation of the model involved in proton-conduction mechanism and the state of water in the membrane. (a) SPAEEKK membrane; (b) SPAEEKK/silica hybrid membrane.

effect of the vehicle mechanism decreases. To maintain the proton conductivity with increasing temperature, the decrease in the effect of the vehicle mechanism must be compensated by an increase in the effect of the Grotthus mechanism. This compensation effect in Nafion is insufficient to maintain the proton conductivity at high temperature because of membrane dehydration due to a higher fraction of freezing bound and free water. The compensation effect is more dependent on the fraction of non-freezing bound water rather than that of freezing bound and free water. Therefore, proton-conducting membranes for use at elevated temperatures, where evaporation would occur, require maintaining water content by means of a high fraction of non-freezing bound water. Table 2 lists the ratio of [Bound water]/[Total water]. The ratio increased with increasing TEOS content.

As shown in Fig. 7, the proton conductivity increased with TEOS content at all temperature conditions. This suggests that the silica doped in the membrane has an effect on improving the formation of proton-conduction pathways due to molecular water absorption. That is, new proton conduction due to the presence of the silica has a probable mechanism associated with proton hopping between SiOH and water molecules [28]. Nogami et al. reported that the dissociated proton moves to a water molecule bound with the SiOH bond, forming the activated $\text{H}_2\text{O}:\text{H}^+$ state ($\text{SiOH}-\text{H}_2\text{O} \rightarrow \text{SiO}^- + \text{H}^+:\text{H}_2\text{O}$) [28]. The proton from the activated $\text{H}_2\text{O}:\text{H}^+$ state dissociates to form a new activated state with a neighboring H_2O . Therefore, the proton conductivity increases due to the synergistic effect between the hydrated sulfonic group and the hydrated

silica particle-absorbed water molecules. It is probable that protons attached to protogenic surface functional groups of $\equiv\text{SiOH}$ participate in the proton-conduction process via the Grotthus mechanism [35]. The H_3PO_4 -doped membranes show somewhat higher proton conductivities compared with H_3PO_4 -free membranes as shown in Fig. 7. Table 2 shows that the water contents of the H_3PO_4 -doped membrane are somewhat higher than that of H_3PO_4 -free hybrid membranes. The introduction of H_3PO_4 enhanced the membrane

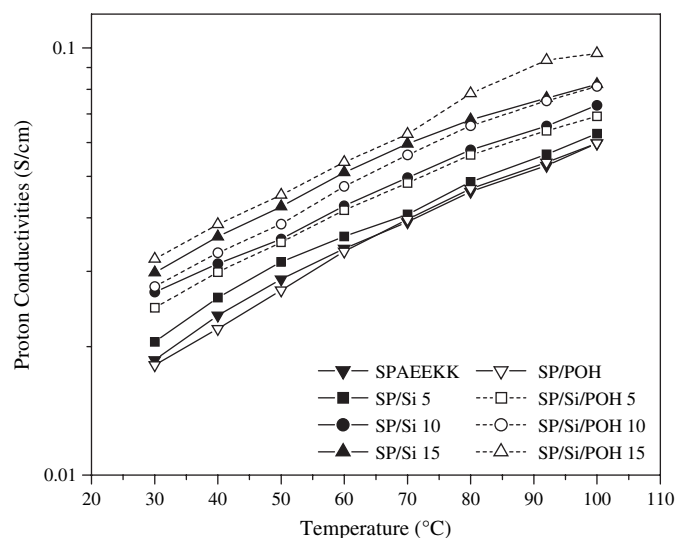


Fig. 7. Proton conductivity of SPAEEKK copolymers.

hydrophilicity due to the hydrogen bonding with water. These water molecules have an effect on forming the pathway for proton transport. It has been reported that the P–OH bonds increase proton conductivity, because of their strong hydrogen bonding with water molecules [27].

Fig. 8 shows the methanol permeabilities of H_3PO_4 -free and H_3PO_4 -doped hybrid membranes. The methanol permeability decreased with increasing TEOS content and increased with increasing temperature. It is known that methanol permeates through hydrophilic ionic channels and that protons are transported by hopping between ionic sites due to hydrogen bonding as well as through ionic channels. Thus, as shown in Fig. 6, the methanol permeability depends more on the size of the ionic channels than the proton conductivity does. Therefore, it could be explained that the methanol permeability decreases due to the silica particles acting as materials for blocking the methanol transport while the proton conductivity should remain largely unchanged.

The methanol permeabilities of the membranes decreased in the same order of ratio [Free]/[Total] as shown in Fig. 8 and Table 2. In addition, the methanol permeabilities of H_3PO_4 -doped membrane are higher than that of H_3PO_4 -free hybrid membranes that have lower ratios of [Free]/[Total]. Therefore, it is logical to surmise that the free water in the membrane contributes to the methanol permeability. The silica particles in the membrane were used as materials for methanol transport blocking and for forming the proton transport pathways due to molecular water absorption.

Fig. 9 shows the proton conductivities and methanol permeabilities of hybrid membranes and Nafion 117 at 30 and 80 °C. Generally, the proton conductivity has a strong trade-off relationship with the methanol permeability [12]. A target membrane would be located in the upper left-hand corner. Fig. 9 shows that the hybrid membranes (SP/Si series, marked 1 and 3) have a favorable trend, compared with a membrane that does not contain any silica. In addition, the SP/Si/POH series (marked 2 and 4) membranes show a more vertical trend. Therefore, the H_3PO_4 -doped membrane improves the

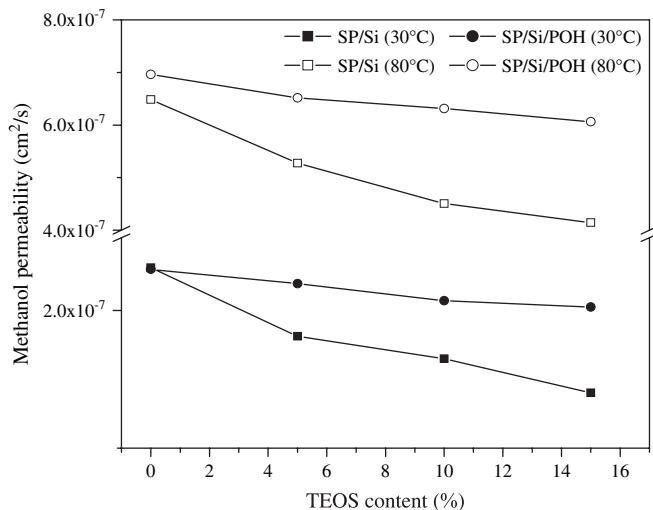


Fig. 8. Methanol permeabilities of SPAEEKK copolymers.

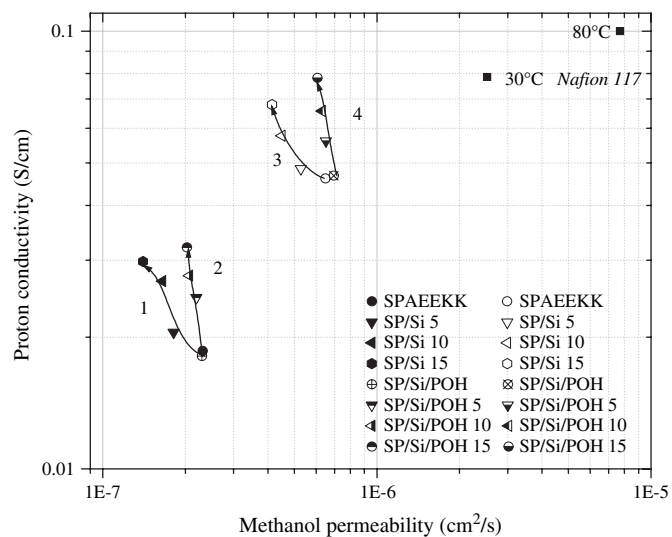


Fig. 9. Proton conductivities versus methanol permeabilities (1: SP/Si series at 30 °C, 2: SP/Si/POH series at 30 °C, 3: SP/Si series at 80 °C, 4: SP/Si/POH series at 80 °C).

proton conductivity, while the methanol permeability remains unchanged.

4. Conclusions

Sulfonated poly(arylene ether ether ketone ketone) (SPAEEKK) copolymer containing pendant sulfonic acid group ($\text{SC} = 0.67$) was synthesized from commercially available monomers such as sodium 6,7-dihydroxy-2-naphthalene-sulfonate (DHNS), 1,3-bis(4-fluorobenzoyl)-benzene (BFBB), and hexafluorobisphenol A (6F-BPA) in NMP at 180 °C. From SPAEEKK, a series of hybrid membranes incorporating different amounts of silica nanoparticles were prepared using the sol–gel reaction with tetraethyl orthosilicate (TEOS). The hybrid membranes were investigated in the un-doped or the H_3PO_4 -doped state.

The proton and methanol transport behavior of the SPAEEKK/silica hybrid membranes and H_3PO_4 -doped hybrid membranes is correlated to the state of water. An improvement in membrane properties is ascribed to a uniform distribution of the nanosized silica particles and H_3PO_4 doping in the membrane matrix. The silica has an effect on the state of water in the membranes. The $\equiv\text{SiOH}$ groups of silica provide strong hydrogen bonding sites in the hybrid membranes. Thus the ratio of bound water to free water increased with silica content. The hybrid membrane improved the retention of water molecules at elevated temperatures and thus proton conductivity was maintained. The proton conductivities of the H_3PO_4 -free and H_3PO_4 -doped hybrid membranes were in the range from 0.02 to 0.082 S/cm and from 0.024 to 0.097 S/cm, respectively. The methanol permeabilities of the hybrid membranes ranged between 1.4×10^{-7} and 6.9×10^{-7} cm^2/s . In comparison with Nafion 117 with a proton conductivity and methanol permeability at 80 °C of 0.1 S/cm and 7.7×10^{-6} cm^2/s , respectively, an SP/Si/POH 15 hybrid membrane had values of 0.078 S/cm and 6.06×10^{-7} cm^2/s . The methanol permeability

was 92.1% lower than Nafion. At 30 °C, the conductivity and permeability values of Nafion 117 were 0.078 S/cm and 2.52×10^{-6} cm²/s, respectively; while an SP/Si/POH 15 hybrid membrane had values of 0.032 S/cm and 2.02×10^{-7} cm²/s, with permeability being 92% lower. These hybrid membranes are potential candidates for polymer electrolytes for DMFC and PEMFC applications.

Acknowledgements

This work was supported by the National Research Council of Canada Fuel Cell program; funded through the Technology and Innovation Research and Development initiative.

References

- [1] Arico AS, Creti P, Antonucci PL, Cho J, Kim H, Antonucci V. *Electrochim Acta* 1998;43:3719.
- [2] Rhim JW, Park HB, Lee CS, Jun JH, Kim DS, Lee YM. *J Membr Sci* 2004;238:143.
- [3] Gierke TD, Munn GE, Wilson FC. *J Polym Sci Part B Polym Phys* 1981;189:1678.
- [4] Heitner-Wirguin C. *J Membr Sci* 1996;120:1.
- [5] Kim YS, Wang F, Hickner M, McCartney S, Hong YT, Harrison W, et al. *J Polym Sci Part B Polym Phys* 2003;41:2816.
- [6] Yeo SC, Eisenberg A. *J Appl Polym Sci* 1977;21:875.
- [7] Yeo RS, Cheng CH. *J Appl Polym Sci* 1986;32:5733.
- [8] Nunes SP, Ruffmann B, Rikowski E, Vetter S, Richau K. *J Membr Sci* 2002;203:215.
- [9] Kim YS, Dong L, Hickner MA, Pivovar BS, McGrath JE. *Polymer* 2003;44:5729.
- [10] Mauritz KA, Stefanithis ID, Davis SV, Scheetz RW, Pope RK, Wilkes GL. *J Appl Polym Sci* 1995;55:181.
- [11] Deng Q, Moore RB, Mauritz KA. *J Appl Polym Sci* 1998;68:747.
- [12] Kim DS, Park HB, Rhim JW, Lee YM. *J Membr Sci* 2004;240:37.
- [13] Kuo PL, Chen WF, Liang WJ. *J Polym Sci Part A Polym Chem* 2005;43:3359.
- [14] Xing P, Robertson G, Guiver MD, Mikhailenko SD, Wang K, Kaliaguine S. *J Membr Sci* 2004;229:95.
- [15] Karlsson LE, Jannasch P. *Electrochim Acta* 2005;50:1939.
- [16] Ma YL, Wainright JS, Litt MH, Savinell RF. *J Electrochem Soc* 2004;151:A8.
- [17] Wang L, Meng YZ, Wang SJ, Li XH, Xiao M. *J Polym Sci Part A Polym Chem* 2005;43:6411.
- [18] Chen YL, Meng YZ, Hay AS. *Polymer* 2005;46:11125.
- [19] Chen YL, Meng YZ, Hay AS. *Macromolecules* 2005;38:3564.
- [20] Wang L, Meng YZ, Wang SJ, Hay AS. *J Polym Sci Part A Polym Chem* 2004;42:1779.
- [21] Kreuer KD. *J Membr Sci* 2001;185:29.
- [22] Lafitte B, Karlsson LE, Jannasch P. *Macromol Rapid Commun* 2002;23:896.
- [23] Gao Y, Robertson GP, Guiver MD, Mikhailenko SD, Li X, Kaliaguine S. *Macromolecules* 2004;37:6748.
- [24] Kim DS, Robertson GP, Guiver MD, Lee YM. *J Membr Sci* 2006;281:111.
- [25] Carrette N, Tricoli V, Picchioni F. *J Membr Sci* 2000;166:189.
- [26] Wang F, Chen T, Xu J. *Macromol Chem Phys* 1998;199:1421.
- [27] Nogami M, Nagao R, Wong C, Kasuga T, Hayakawa T. *J Phys Chem B* 1999;103:9468.
- [28] Nogami M, Nagao R, Wong C. *J Phys Chem B* 1998;102:5772.
- [29] Zhang Y, Wang M. *Mater Sci Eng* 1999;B67:99.
- [30] Huang JC, Zhu ZK, Yin J, Zhang DM, Qian XF. *J Appl Polym Sci* 2001;79:794.
- [31] Liu YL, Hsu CY, Wei WL, Jeng RJ. *Polymer* 2003;44:5159.
- [32] Kim YS, Dong L, Hickner MA, Glass TE, Webb V, McGrath JE. *Macromolecules* 2003;36:6281.
- [33] Lee CH, Park HB, Chung YS, Lee YM, Freeman BD. *Macromolecules* 2006;39:755.
- [34] Kreuer KD. *Chem Mater* 1996;8:610.
- [35] Krishnan P, Park JS, Kim CS. *J Membr Sci* 2006;279:220.